JOURNAL OF MATERIALS SCIENCE **38** (2003) 3473–3478

Synthesis of nanocrystalline MoN from a new precursor by TPR method

SHUTAO WANG, XIONG WANG, ZUDE ZHANG*, YITAI QIAN
Department of Chemistry, University of Science and Technology of China, Hefei, Anhui 230026, People's Republic of China
E-mail: zzd@ustc.edu.cn

Molybdenum nitride (MoN) nanoparticles with high BET surface area (S_{BET} = 351.0352 m^2/g) have been successfully obtained from ammonium polymolybdate, $(NH_4)_6Mo_7O_{24}$. Differential thermal analysis (DTA), thermogravimetric analysis (TGA) and X-ray powder diffraction (XRD) analysis were used to investigate the effect of water in the precursor. X-ray photoelectron spectroscopy (XPS) was used to determine the empirical formula of the product. Also, MoN nanorods with high aspect ratio have been prepared using Al_2O_3 template. XRD, transmission electron microscopy (TEM) and high resolution transmission electron microscopy (HRTEM) were used to characterize the structure of the nanorods.
© *2003 Kluwer Academic Publishers*

1. Introduction

In recent years, great attention has been paid to MoN for its excellent heterogeneous catalytic activity in many fields, such as ammonia synthesis [1–3], hydrodenitrogenation (HDN) [4–7], hydro-desulfurization (HDS) [8–10], and isomerization of certain hydrocarbons [8, 9, 11]. MoN also has attractive mechanical, electrical and magnetic properties, and is suitable for applications in cutting tools, wear-resistant parts, high temperature materials and superconductors [12]. Synthesis of other important materials, such as carbides, borides, etc. can also use MoN as a precursor [13].

Conventionally MoN is synthesized mainly with molybdenum trioxide (MoO_3) precursor [11, 14]. For mass preparation of MoN, however, hindered heat transfer problems caused by endothermic NH_3 decomposition and H_2O vapor formation [14] exist in these approaches. So it is necessary to investigate the possibility using other gas phase chemistry or solid precursors [15]. Kojima and co-workers have prepared cobalt molybdenum bimetallic nitride (Co_3Mo_3N) from $CoMoO_4$ or $CoMoO_4{\cdot}nH_2O$ [16, 17]. The hydrate precursor was heated at 423 K or 1073 K before nitridation, which inevitably altered the state of water. But few publications about the influence of water are reported [18, 19]. Presented here is a study on synthesis of MoN with $(NH_4)_6Mo_7O_{24}$ precursor at various temperatures by temperature-programmed reaction (TPR) method. By means of thermo-analytical techniques (DTA and TGA), the effect of water in the precursor is discussed.

High specific surface area is indispensable to catalyst. Since Al_2O_3 template is known for having very high surface area [20], MoN prepared by alumina-template method may have significantly high surface area. MoN hollow fibers have been prepared from needle sulfide precursor [21]. Both hollow and solid fibers have been prepared with Al_2O_3 template [22, 23]. Furthermore, alumina-supported nitride is reported to exhibit higher catalytic activity than corresponding sulfide [8]. With Al_2O_3 template nanofibers of MoN have been obtained and control over the shape and size distribution of the product has been achieved in our experiments.

The reaction of MoO_3 with NH_3 is revealed to be topotactic [10, 14], which means the solid product has a well-defined crystallographic orientation in comparison with the starting material. Possible topotactic relationships between the reactants and the products need to be thoroughly examined in future.

2. Experimental

Ammonium polymolybdate (VI) tetrahydrate, $(NH_4)_6Mo_7O_{24}{\cdot}4H_2O$, was used as the source of molybdenum. For comparison, it was used as received (commercial sources, analytical grade) or heated at about 423 K to remove some water before reaction.

$(NH_4)_6Mo_7O_{24}$ supported on Al_2O_3(S_{BET} = 328.52 m^2/g) was prepared as follows [24]: 5 g $(NH_4)_6Mo_7O_{24}{\cdot}4H_2O$ was dissolved in 15 ml H_2O, and then Al_2O_3 was impregnated into the solution. The mixture was stirred for 1 h before H_2O was evaporated at 423 K in the air.

MoN was obtained following a procedure reported elsewhere [21, 24]. The precursor was placed in a quartz reactor inside a tube furnace. NH_3 (50 $ml{\cdot}min^{-1}$) was introduced into the reactor to expel air before reaction. The precursor was heated to 673 K at 10 $K{\cdot}min^{-1}$,

*Author to whom all correspondence should be addressed.

then to 873 K, 1023 K, and 1073 K at 3 K·min^{-1}, respectively. A thermocouple and a programmed AI-808P Maxonic automatic controller were used to monitor and control temperature. The reactor was kept at the final temperature for 5 or 12 h. The sample was then naturally cooled to room temperature in flowing NH_3 [10, 11, 25]. Drops of condensed water remained at the exit of the reactor. As expected, white $(NH_4)_6Mo_7O_{24}$ and $(NH_4)_6Mo_7O_{24}/Al_2O_3$ turned into black MoN, respectively.

To determine the influence of water, $(NH_4)_6Mo_7O_{24}\cdot 4H_2O$ was analyzed by DTA, TGA, and XRD both before and after heat treatment. DTA was performed using a CRY-2 thermal analyzer. TGA was performed using a WRT-3 thermogravimetric analyzer. Both thermal analytical techniques were accomplished under nitrogen atmosphere with a ramping rate of 10 K·min^{-1} from room temperature to 1073 K.

XRD was conducted on a Rigaku D/MAX-γA X-ray diffractometer with a graphite-monochromatized Cu K_α radiation ($\lambda = 1.5418$ Å). Diffraction data were collected by step scanning over the 2θ range from 20° to 70° with a step width of 0.06°.

TEM images were taken with a Hitachi H-800 transmission electron microscope, and HRTEM images with a JEOL-2010 high resolution transmission electron microscope, both using an accelerating voltage of 200 kV. Prior to measurement, supported product was immersed in 1.0 M NaOH solution to remove Al_2O_3. The remaining black solid was collected and observed.

XPS spectra were recorded on a VG ESCALAB MK-II spectrometer, using nonmonochromatized Mg K_α radiation as excitation source.

The S_{BET} value of the samples was determined by N_2 adsorption BET method. The pore volume distribution of Al_2O_3 was measured from N_2 desorption isotherm using the BJH method. The samples were outgassed at 573 K for 12 h before analysis on a Micromeritics ASAP 2000 analyzer.

3. Results and discussion

It is well known that there are three kinds of water in crystal [26]: adsorbed water, crystal water, and constitution water. Due to various interactions between its parent crystal structure and each kind of water, the dehydration process goes through several steps. The effect of water is particularly dramatic as the XRD patterns show in Fig. 1. At 1073 K, nitride can be obtained from both heated (sample e) and unheated precursors (sample c). But when temperature decreases to 873 K, nitride appears only in the case of heated precursor (sample b). In contrast to those of sample c, the diffraction peaks of sample e are sharper, indicating better crystallization. From the above results, it is concluded that after pretreatment of the precursor, nitridation temperature can be reduced and the degree of crystallization can be improved.

Fig. 2 shows the XRD patterns of the precursor. Obvious phase transformation occurs after heat treatment. Heated precursor (Fig. 2a) is indexed as $(NH_3)_4Mo_5O_{15}\cdot 2H_2O$ (JCPDS card No. 21-971). Hydrate precursor (Fig. 2b) is indexed as $(NH_4)_6Mo_7O_{24}\cdot 4H_2O$

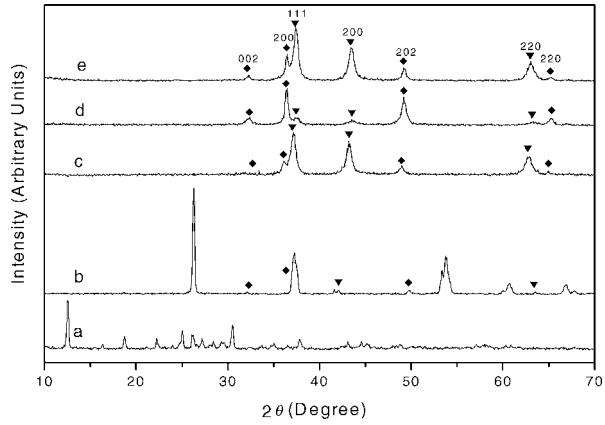

Figure 1 The XRD spectra of sample a–e (a prepared via unheated precursor at 873 K for 5 h; b prepared via heated precursor at 873 K for 5 h; c prepared via unheated precursor at 1073 K for 5 h; d prepared via heated precursor at 1023 K for 12 h; e prepared via heated precursor at 1073 K for 5 h) (▼, cubic phase; ♦, hexagonal phase).

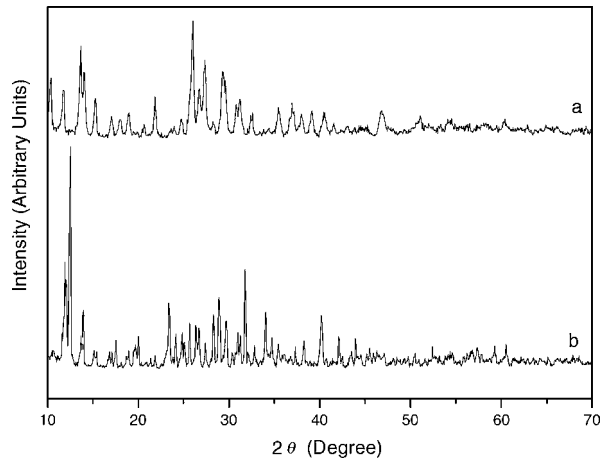

Figure 2 The XRD spectra of the precursor (a heated precursor; b unheated precursor).

(JCPDS card No. 27-1013 and No. 70-1707). Since constitution water cannot be vaporized at 423 K, and physisorbed water can be vaporized at 393–423 K, water lost at the pretreatment temperature consists of both crystal and physisorbed water.

The DTA result of the precursor is shown in Fig. 3. There are four endothermic regions for hydrate precursor (Fig. 3b). The first region is situated at around 409.6 K, the second around 515.8 K, and the third around 601.7 K. These three regions are the result of dehydration of the hydrate. The fourth and most intense

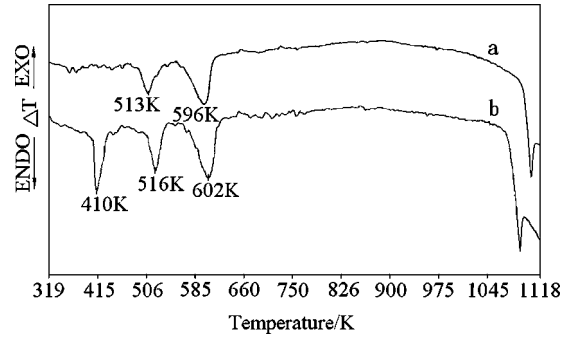

Figure 3 The DTA result of the precursor (a heated precursor; b unheated precursor).

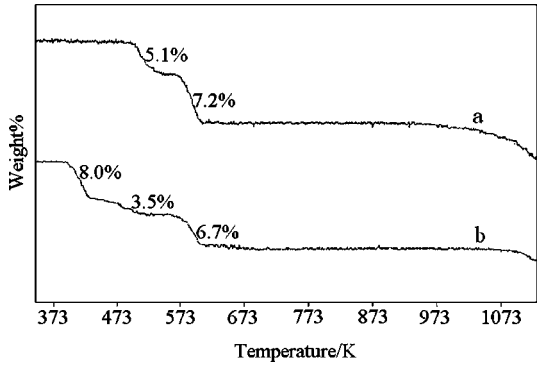

Figure 4 The TGA result of the precursor (a heated precursor; b unheated precursor).

peak around 1073 K, at which temperature nitridation reaction takes place, suggests pyrolytic decomposition of the precursor. All the physisorbed water can be removed by heat treatment, so there is no endothermic peak around 410 K in Fig. 3a. The peak around 513 K is attributed to the removal of crystal water, which has not been totally removed by pretreatment. Both Fig. 3a and b show that most of the constitution water is vaporized when the temperature is higher than 773 K [18]. The areas of the endothermic regions of the heated precursor are obviously smaller than those of the unheated one. This suggests that less thermal energy is needed for the decomposition of heated precursor. Nitridation temperature may be reduced by heat pretreatment. This conclusion is consistent with the above XRD result.

The overall nitridation reaction is expressed as follows:

$$2(NH_4)_6Mo_7O_{24}(s) + 16NH_3(g) = 14MoN(s) + 48H_2O(g) + 7N_2(g)$$

Following the law of mass action, the reaction would be inhibited under increased partial pressure of water. On the other hand, H_2O may oxidize low valence state Mo in MoN. Heated precursor contains less water than hydrate precursor. Constitution water may bring some vacancy defects, which can be easily attacked by the nitrogen of decomposed NH_3 [7]. So the existence of constitution water in heated precursor becomes a dominant promoting factor in nitridation process [18]. At the same time, potential hydrothermal sintering is also reduced.

The TGA result (Fig. 4) provides further information about the precursor. All the dehydration intervals of the TGA curves are in agreement with the endothermic regions of the DTA data. The change of weight around 1073 K also implies the occurrence of nitridation reaction. It is shown again that nitridation of $(NH_4)_6Mo_7O_{24}$ will be realized much more easily after heat treatment of the precursor.

Fig. 1 shows the XRD patterns of products obtained at various reaction conditions. Unsupported samples are identified as MoN in Fig. 1c–e. All the products include both hexagonal and cubic phases. The nitride prepared at 1023 K is mainly hexagonal phase (sample d, JCPDS card No. 25-1367). When the reaction temperature is increased to 1073 K, cubic phase is predominant (sample c and e, JCPDS card No. 25-1366). There is a shift of the diffraction peaks for the same phase in different samples. Correlative change in lattice constant and corresponding reaction conditions are summarized in Table I. No impurities such as MoO_2 or Mo are detected.

The average crystallite size is calculated using the Scherrer equation, $d_c = K\lambda/B\cos\theta$, where K is a constant (taken here to be 0.9), λ the wavelength of the radiation (1.5418 Å), B the corrected peak width at half maximum intensity, and θ the Bragg angle of the diffraction peak. The calculated results are also listed in Table I. With increasing reaction temperature, the average size of nitride decreases from 21.8 nm (sample b) to 18.8 nm (sample d) and 14.6 nm (sample e). The size of sample a and sample b is 22.7 nm and 21.8 nm, respectively. The size of sample c and sample e is 16.2 nm and 14.6 nm, respectively. This indicates that heated precursor results in a smaller size of the final nanoparticles than unheated precursor at the same reaction conditions.

Analysis of XPS spectra (Fig. 5) exhibits a Mo:N ratio of 0.941, which approximately corresponds to the stoichiometric ratio of MoN. There are three peaks of Mo3d in Fig. 5a, indicating the existence of two valence states of molybdenum. The binding energy at 229 eV, close to the corresponding value of $Mo3d_{5/2}$ in Mo_2C (228.6 eV) [27], is attributed to Mo (II). The peak at 235.1 eV is attributed to Mo (VI). The peak of sample e at 229 eV becomes stronger at increased temperature, while the peak at 235.1 eV changes in a contrary direction. So more nitride is prepared accompanying the reduction of Mo (VI). Oxidation of low valence state of Mo leads to the existence of Mo (VI) in both of the samples. But no peaks of oxide are observed from the XRD patterns. It can be explained from two aspects: First,

TABLE I The reaction conditions, lattice constant, and average crystallite size

	Reaction conditions			Lattice constant			
					Hexagonal		
	Temperature (K)	Time (h)	Precursor	Cubic a (Å)	a (Å)	c (Å)	Crystallite size d (nm)
Sample a	873	5	Unheated	–	–	–	22.7
Sample b	873	5	Heated	–	–	–	21.8
Sample c	1073	5	Unheated	4.186	5.813	5.556	16.2
Sample d	1023	12	Heated	4.088	5.721	5.602	18.8
Sample e	1073	5	Heated	4.164	5.738	5.608	14.6
Theoretical value	–	–	–	4.163	5.725	5.608	–

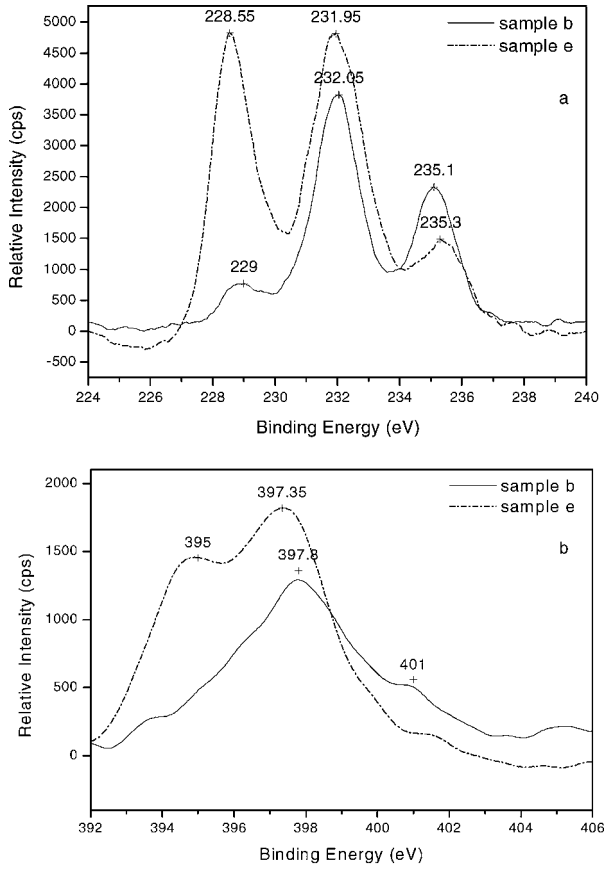

Figure 5 XPS spectra of MoN prepared at different temperatures: (a) XPS of Mo (3d) of MoN and (b) XPS of N (1s) of MoN.

the amount of Mo (VI) is below the resolution limit of XRD measurement; second, Mo (VI) which is mainly in the form of oxynitride or amorphous oxide [28], has not completely crystallized at the surface layer. Fig. 5b shows the XPS spectra of N (1s) of the products. The binding energy of N1s in sample b is 397.8 eV, close to that of N1s in BN (397.9 eV), suggesting formation

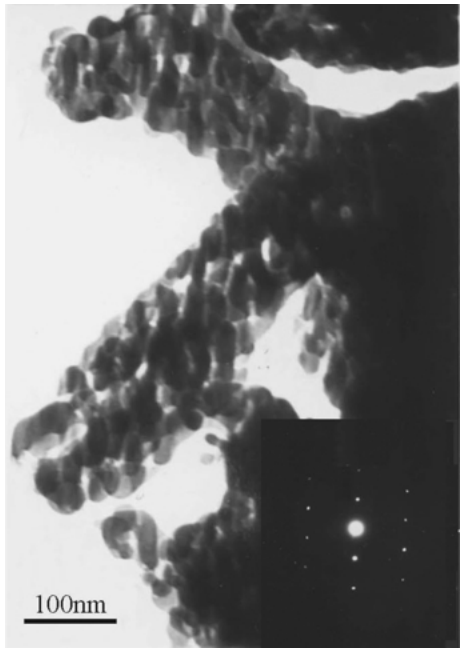

Figure 6 TEM image of MoN particles (prepared via heated precursor at 1073 K for 5 h).

Figure 7 TEM image of MoN nanorods (prepared via Al_2O_3/precursor at 953 K for 5 h).

of Mo–N bond. The peak around 401 eV is caused by chemisorbed NH_3, the amount of which is reduced significantly in sample e. At 1073 K, the peak of N1s in sample b (397.8 eV) shifts to 397.35 eV, and a new peak at 395 eV appears, suggesting formation of nitride. It is therefore concluded that the yield of nitride can be increased by high reaction temperature [29, 30].

The S_{BET} value of sample e is 351.04 m^2/g. TEM image (Fig. 6) shows that it consists of agglomerates of irregular fine particles. MoN fibers are also observed for Al_2O_3 supported sample, as evidenced in Fig. 7. The

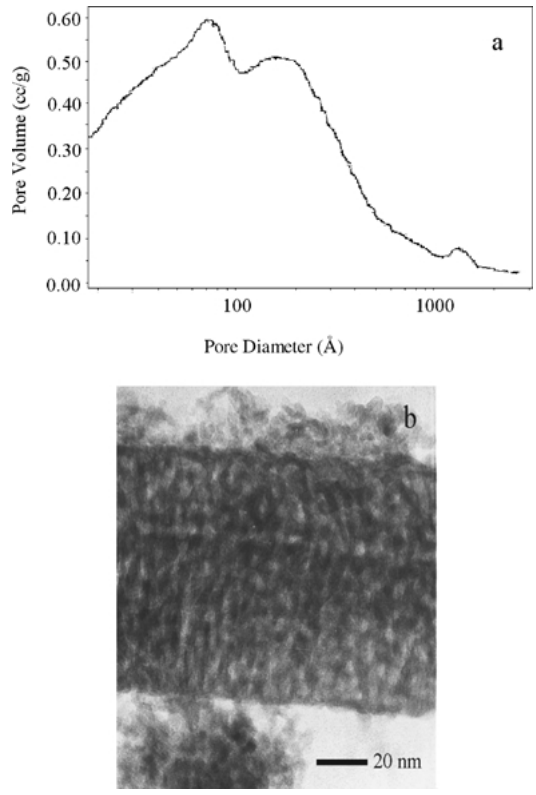

Figure 8 (a) dv/dlog (D) desorption pore volume plot of Al_2O_3 and (b) HRTEM image of Al_2O_3.

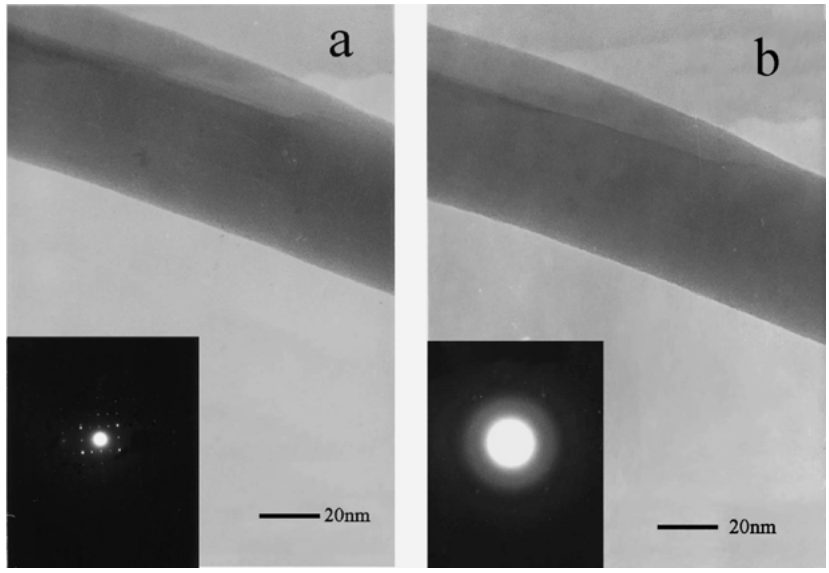

Figure 9 HRTEM images of MoN nanorod (prepared via Al_2O_3/precursor at 953 K for 5 h): (a) quickly shot the moment the nanorod subjected to electron radiation, the SAED pattern is discernable and (b) after the radiation of electron, obvious bend occurred and the SAED diffraction spots disappeared.

S_{BET} value of the fibers is 13.76 m^2/g. These high aspect ratio (length/diameter) fibers are solid, about 30–65 nm in diameter and 1.18 μm in length. These non-uniform diameters are caused by the irregular pore diameters of Al_2O_3 template. Fig. 8a shows the dv/dlog(D) desorption pore volume plot of Al_2O_3. And Fig. 8b shows the morphology of Al_2O_3 template. The plugs transecting MoS_2 tubule in a similar procedure [24] have not been found. These may result from complex interactions among the precursors, the templates, and the impregnation solvents. As the HRTEM photographs show in Fig. 9, these fibers change from single crystallite to amorphous phase when exposed to intensitive irradiation of electron beam, and the selected-area electron diffraction spots (SAED) gradually vanish. At 953 K, some constitution water still remains in the structure. It is also possible that the precursor has not been completely nitrided. Zhang *et al*. [31] reported the existence of H_xMoO_3 as an intermediate. Under the high energy irradiation of electron beam, the intermediates may decompose, and constitution water may be released from the crystals, resulting in collapse of the crystal structure. During this process, the intensity of the SAED diffraction spots becomes gradually fuzzy.

4. Conclusion

- As a conclusion, $(NH_4)_6Mo_7O_{24}$ is an efficient and practical precursor for preparation of MoN. With this new precursor, nanocrystalline MoN was synthesized by TPR method under flowing ammonia.
  - Water plays an important role in the nitridation process, whether as a by-product of nitridation or in the form of crystal or constitution water.
  - MoN nanorods with diameter of 30 nm and length of 1.18 μm are synthesized. Control over the shape and the size of the product has been realized with Al_2O_3 template.
  - Further research of the catalytic properties of MoN prepared this way, preparation of phase-pure MoN and optimization of the reaction conditions are in progress.

Acknowledgments

The financial support from the National Natural Science Research Foundation of China is gratefully acknowledged.

References

1. L. VOLPE and M. BOUDART, *J. Phys. Chem.* **90** (1986) 4874.
2. R. KOJIMA and K. AIKA, *Appl. Catal. A-Gen.* **219** (2001) 141.
3. *Idem.*, *ibid.* **218**(1/2) (2001) 121.
4. S. RAMANATHAN and S. T. OYAMA, *J. Phys. Chem.* **99** (1995) 16365.
5. M. NAGAI and T. MIYAO, *Catal. Lett.* **15** (1992) 105.
6. S. Z. LI, J. S. LEE, T. HYEON and K. S. SUSLICK, *Appl. Catal. A-Gen.* **184**(1) (1999) 1.
7. M. NAGAI, Y. GOTO, A. MIYATA, M. KIYOSHI, K. HADA, K. OSHIKAWA and S. OMI, *J. Catal.* **182**(2) (1999) 292.
8. M. NAGAI, T. MIYAO and T. TSUBOI, *Catal. Lett.* **18** (1993) 9.
9. J. TRAWCZYŃSKI, *Catal. Today* **65**(2–4) (2001) 343.
10. E. J. MARKEL, S. E. BURDICK, M. E. LEAPHART II and K. L. ROBERTS, *J. Catal.* **182**(1) (1999) 136.
11. M. K. NEYLON, S. CHOI, H. KWON, K. E. CURRY and L. T. THOMPSON, *Appl. Catal. A-Gen.* **183**(2) (1999) 253.
12. D. A. PAPACONSTANTOPOULOS and W. E. PICKETT, *Phys. Rev.* B **31**(11) (1985) 7093.
13. L. VOLPE and M. BOUDART, *J. Solid State Chem.* **59** (1985) 348.
14. *Idem.*, *ibid.* **59** (1985) 332.
15. R. S. WISE and E. J. MARKEL, *J. Catal.* **145** (1994) 335.
16. R. KOJIMA and K. AIKA, *Appl. Catal. A-Gen.* **215**(1/2) (2001) 149.
17. *Idem.*, *Chem. Lett.* (2000) 514.
18. J. H. KIM and K. L. KIM, *Appl. Catal. A-Gen.* **181**(1) (1999) 103.
19. M. F. DANIEL, B. DESBAT, J. C. LASSEGUES, B. GERAND and Z. M. FIGLAR, *J. Solid State Chem.* **67** (1987) 235.
20. C. A. FOSS, G. L. HORNYAK, J. A. STOCKERT and C. R. MARTIN, *J. Phys. Chem.* **96** (1992) 7497.

21. L. RENMAO, Z. ZUDE and Q. YITAI, Manuscript in preparation.
22. C. M. ZELENSKI and P. K. DORHOUT, *J. Amer. Chem. Soc.* **120**(4) (1998) 734.
23. Y. K. ZHOU and H. L. LI, *J. Mater. Chem.* **12**(3) (2002) 681.
24. M. Z. CATHERINE and K. D. PETER, *J. Amer. Chem. Soc.* **120** (1998) 734.
25. M. CHE, J. C. MCACTEER and A. J. TENCH, *Chem. Phys. Lett.* **31** (1975) 145.
26. Y. SHUZHEN and Z. HEPING, in "Measurement of Inorganic Non-metal Materials" (Wuhan, University of Industry of Wuhan, 1990).
27. D. BRIGGS and M. P. SEAH, in "Practical Surface Analysis," 2nd ed., Vol. 1 (Wiley, New York, 1990).
28. Z. YAOJUN, J. CHUNXIN, L. XINSHENG, S. SHISHAN, X. QIN and ZH. SHUXIAN, *Chinese J. Chem. Phys.* **10**(6) (1997) 540.
29. H. KWON, S. CHOI and L. T. THOMPSON, *J. Catal.* **184**(1) (1999) 236.
30. R. KAPOOR and S. T. OYAMA, *J. Solid State Chem.* **99** (1992) 303.
31. Z. YAOJUN, X. QIN, R. INMACULADA and G. ANTONIO, *Mater. Res. Bull.* **34**(1) (1999) 145.

Received 29 July 2002
and accepted 4 April 2003